INTRODUCTION

Nanotechnology, an interdisciplinary research field involving chemistry, engineering, biology, and medicine, has great potential for early detection, accurate diagnosis, and personalized treatment of cancer. [1]

Nanoparticles are typically smaller than several hundred nanometers in size, comparable to large biological molecules such as enzymes, receptors, and antibodies. With the size of about one hundred to ten thousand times smaller than human cells, these nanoparticles can offer unprecedented interactions with biomolecules both on the surface of and inside the cells, which may revolutionize diagnosis and treatment of diseases. [2]

A nanoparticle is the most fundamental component in the fabrication of a nanostructure, and is far smaller than the world of everyday objects that are described by Newton ' s laws of motion, but bigger than an atom or a simple molecule that are governed by quantum mechanics. [3]

In general, the size of a nanoparticle spans the range between 1 and 100 nm. Metallic nanoparticles have different physical and chemical properties from bulk metals (e.g., lower melting points, higher specific surface areas, specific optical properties, mechanical strengths, and specific magnetizations), properties that might prove attractive in various industrial applications. However, how a nanoparticle is viewed and is defined depends very much on the specific application. Of particular importance, the optical property is one of the fundamental attractions and a characteristic of a nanoparticle. For example, a 20-nm gold nanoparticle has a characteristic wine red color. [3]

A silver nanoparticle is yellowish gray. Platinum and palladium nanoparticles are black. Not surprisingly, the optical characteristics of nanoparticles have been used from time immemorial in sculptures and paintings even before the 4th century AD. The most famous example is the Lycurgus cup (fourth century AD). [3]

This extraordinary cup is the only complete historic example of a very special type of glass, known as dichroic glass, that changes color when held up to the light. The opaque green cup turns to a glowing translucent red when light is shone through it internally (i.e., light is incident on the cup at 90° to the viewing direction). Analysis of the glass revealed that it contains a very small quantity of tiny (~ 70 nm) metal crystals of Ag and Au in an approximate molar ratio of 14: 1, which give it these unusual optical properties. It is the presence of these nanocrystals that gives the Lycurgus Cup its special color display. The reader can marvel at the cup now in the British Museum. [3]

Until the Middle Ages, the reputation of soluble gold was based mostly on its fabulous curative powers of various diseases, for example, heart and venereal diseases, dysentery, epilepsy, and tumors; it was also used in the diagnosis of syphilis. [4]

Francisci Antonii in 1618[3] has published the first book on colloidal gold. This book includes considerable information on the formation of colloidal gold sols and their medical uses, including successful practical cases. The book noted that soluble gold appeared around the fifth or fourth century B.C. in Egypt and China. On the other hand, industrial manufacturing of stained glass with colloidal particles was established by Kunckel in the

seventeenth century (1676). [3] He concluded that gold must be present in aqueous gold solutions to a degree of contamination such that it is not visible to the human eye. A colorant in glasses, that is, the "Purple of Cassius", was a colloid resulting from the presence of gold particles and tin dioxide and was highly popular in the seventeenth. [3]

Melcher in 1718[3] published a complete treatise on colloidal gold. In the treatise, this philosopher and doctor stated that the use of boiled starch in its drinkable gold preparation noticeably enhanced its stability. These ideas were common in the eighteenth century, as indicated in French chemical dictionary dated 1769. [3], under the heading "or potable" it was said that drinkable gold contained gold in its elementary form, albeit under extreme sub-division suspended in a liquid. In 1794, Fuhlame reported in a book that she had dyed silk with colloidal gold. [3]

Jeremias Benjamin Richters In 1818 [5] suggested an explanation for the differences in color shown by various preparations of drinkable pink or purple gold solutions in that these solutions contained gold in the finest degree of subdivision, whereas yellow solutions were found when the fi ne particles had aggregated.

Michael Faraday in a well-known publication In 1857 [5] reported the formation of deep red solutions of colloidal gold by reduction of an aqueous solution of chloroaurate (AuCl 4) by phosphorus in CS 2 (a two-phase system). He also investigated the optical properties of thin films prepared from dried colloidal solutions and observed reversible color changes of the films upon mechanical compression (from bluish-purple to green). [6]

Since that pioneering work, thousands of scientific papers have been published on the synthesis, modification, properties, and assembly of metal nanoparticles, using a wide variety of solvents and other substrates. [6]

Nanotechnology is easily evident in various old churches. A well-known application of early nanotechnology is the ruby red color that was used for stained glass windows during the Middle Ages, an examples of these applications can be found in glass windows of many Gothic European cathedrals.[6]

These vivid colors which used to stain the glass were controlled by the size and the form (or shape) of the nanoparticles of gold and silver. The relation between particles and their associated colors has been discussed recently by Jin and coworkers [6]

The current technology that deals with nanoparticles, or simply nanotechnology, began from the special optical phenomenon and the establishment of a theory to describe the various physical phenomena that were followed subsequent to the development of analytical instruments. This continues as we speak, with various nanostructures being proposed and discovered, and their applications described. [3]

Industrial production of nanomaterials saw its origins in the twentieth century. For example, nanoparticles of carbon black (tire soot) have been used in the fabrication of rubber tires of automobiles from the beginning of the twentieth century. Pigments such as SiO 2 and TiO 2 have been prepared by a high-temperature combustion method. Since the 1970s, the innovative development of nanoparticles is due to a combination of theory and experiments in the fields of physics, chemistry, materials science, and biosciences. Specific phenomena (chemical properties and physical properties), other than the optical property of

a nanoparticle, have led to new possibilities in various fields. Applications of nanoparticles in various fields require an inexpensive and simple process of synthesizing high quality shaped nanoparticles. [3]

Synthesis of nanoparticles using microwave heating has been on the increase in recent years. Fabrication of high quality nanoparticles can be achieved by simple operations compared with the more conventional nanoparticle synthetic methods. [3]

The well-studied nanoparticles include quantum dots, carbon nanotubes, paramagnetic nanoparticles, liposomes, gold nanoparticles and many others [7]

One of the most promising applications of nanotechnology is in the field of medicine. Indeed, a whole new field of "nanomedicine" is emerging. Nanomedicine has been defined as the monitoring, repair, construction and control of human biological systems at the molecular level using engineered nano devices and nanostructures. It can also be regarded as another implementation of nanotechnology in the field of medical science and diagnostics. [8]

Twenty years from now, nanotechnology will have given us specially engineered drugs that specifically target just the mutant cancer cells in the human body, and leave everything else blissfully alone. Cancer will be a thing of the past. [8]

Applications of nanotechnology in medicine aim to diagnose, drug delivery targeted at specific sites in the body, molecular, radiological imaging and treat diseases by working at the nanometer scale where biological macromolecules exist and operate [9-10]

In the past decade, nanotechnology has emerged as a new and powerful weapon for the detection and treatment of cancer. [9] Nanoparticles have unique and tunable properties [11] when these particles are conjugated to biorecognition molecules; they can home in to a molecular target (such as a cancer marker) and highlight the presence of cancer for use of cancer detection, or deliver a cytotoxic agent for use in targeted therapy [12]

Common deleterious consequences of systemic bio distribution include toxicity to nontarget tissues, difficulty in maintaining drug concentrations within therapeutic windows, and metabolism and excretion of drugs, all of which can reduce efficacy. Drug solubility and cell permeability issues are also common with small molecules and biologics. [13]

Nanotechnology-based delivery systems could mitigate these problems by combining tissue- or organ-specific targeting with therapeutic action. Multifunctional nano-delivery systems could also combine targeting, diagnostic, and therapeutic actions. More than 90 years ago. [8]

Nobel laureate German immunologist Paul Ehrlich proposed the so-called magic bullets artificial biochemical agents that would transport and release drugs at only desired sites in the body. Targeting the delivery of drugs to diseased lesions is one of the important aspects of the drug delivery systems. To convey a sufficient dose of drug to the lesion, suitable carriers of drugs are needed. Although opportunities to develop nanotechnology-based efficient drug delivery systems extend into all therapeutic classes of pharmaceuticals, the development of effective treatment modalities for the respiratory,

central nervous system, and cardiovascular disorders remains a financially and therapeutically significant need. [8]

Many therapeutic agents have not been successful because of their limited ability to reach to the target tissue. In addition, faster growth opportunities are expected in developing delivery systems for anti-cancer agents, hormones, and vaccines owing to safety and efficacy shortcomings in their conventional administration modalities. For example, in cancer chemotherapy, cytostatic drugs damage both malignant and normal cells alike. Thus, a drug delivery strategy that selectively targets the malignant tumor is very much needed. Additional problems include drug instability in the biological milieu and premature drug loss through rapid clearance and metabolism. Similarly, high protein binding of certain drugs such as protease inhibitors limits their diffusion to the brain and other organs. However, nanotechnology for drug delivery applications may not be suitable for all drugs, especially those drugs that are less potent because the higher dose of the drug would make the drug delivery system more massive, which would be difficult to administer. [8]

Drug bioavailability is a related problem with potential nanotechnology solutions. Nanotechnology is opening up new therapeutic opportunities for a large number of agents that cannot be used effectively as conventional oral formulations, due to poor bioavailability. In some cases, reformulation of a drug with smaller particle size may improve oral bioavailability. Nanoparticles formulations provide protection for agents susceptible to degradation or denaturation in regions of harsh pH, and also prolong the duration of exposure of a drug by increasing retention of the formulation through bio adhesion. [8]

Another broad application of nanotechnology is the delivery of antigens for vaccination. Mucosal immunity is extremely important in disease prevention, but continues to be limited by both degradation of the vaccine and limited uptake. Recent advances in encapsulation and development of suitable animal models have demonstrated that micro and nanoparticles are capable of enhancing immunization. It has been shown that M cells in the Peyer's Patches of the distal small intestine are capable of engulfing large microparticles and recent studies have explored the benefits of nano encapsulation. [8]

Treatment for cancer is most effective if the disease is diagnosed early, before it has metastasized or spread beyond the site of the initial tumour. To illustrate: in the United States, the 5-year relative survival rate for localized breast cancer is 97%. If the cancer has spread regionally, the survival rate dips to 78%. Once metastasis has occurred, this survival rate plummets to 23%. The early stages where treatment is most effective, however, are often asymptomatic. Early detection strategies use imaging systems to detect physiological and anatomical changes concomitant with oncogenesis, or molecular probes to detect cancer biomarkers such as proteases, antigens, antibodies, proteins and nucleic acid based markers, Nanoparticles have been used as contrast agents in both strategies.[14]

Another broad application of nanotechnology include: Fluorescent biological labels, bio detection of pathogens, detection of proteins, probing of DNA structure, tissue engineering, tumour destruction via heating (hyperthermia),Separation and purification of biological molecules and cells, MRI contrast enhancement, Phagokinetic studies. [8-15]

Contrast agents are now a standard practice in the field of medical imaging, where they are used to enhance image contrast and improve the visibility of features that would otherwise be difficult to detect. [16]

Current conventional contrast agents for X-ray are based on iodinated small molecules, because among non-metal atoms, iodine has a high X-ray absorption co-efficient. [17] Iodinated compounds, however, allow only very short imaging time due to rapid clearance by the kidney, which can also cause them to have renal toxicity. [18]

Contrast agents for X-rays are based on tri-iodobenzene along with substituents added for water solubility. Diatrizoate, an ionic form, was introduced in 1954, but the high osmolality of this compound (1.57 osm kg-1 for a 300 mg ml-1 solution) was found to be the source of chemotoxicity. In the 1970s, a non-ionic form, iohexol, lowered the osmolality (0.67 osm kg-1), and is still widely used today under the names of OmnipaqueHExypaqueH, and Amersham Health, Amersham, UK (now GE Healthcare). Because osmolality was still excessive, a dimeric form was introduced, iodixanol (AcupaqueH and VisipaqueH, Amersham Health, Amersham, UK (now GE Healthcare); 0.29 osm kg-1). [19]

Intravascular agents based on other mid-Z to high-Z elements have not been successful due to their toxicity, performance, or cost. The low molecular weights of the iodine agents (diatrizoate, 613; iohexol, 821; iodixanol, 1550) affect the rapid renal clearance and vascular permeation, necessitating short imaging times. Intra-arterial catheterisation is therefore commonly needed, but carries the risks of arterial puncture, dislodgement of plaque, stroke, myocardial infarction, anaphylactic shock and renal failure. A further shortcoming of the current agents is in molecular imaging, since their conjugates with antibodies or other targeting moieties fail to deliver iodine to desired sites at detectable concentrations. [19]

Nanoparticle agents continue to receive considerable attention in the medical imaging field for their potential uses contrast agents; they have the advantage of greater biocompatibility and reduced toxicity compared to more conventional chemical agents, present nanoparticles that are under development for this role include gold nanoparticles for X-ray contrast enhancement, magnetic nanoparticles for magnetic resonance imaging (MRI) enhancement, and even hybrid nanoparticles containing iron oxide and gold in a polymer coating, which serve as contrast agents for both computed tomography (CT) and MRI. [20-21]

BASIC CONSIDERATIONS

Radiological Modalities

1. Diagnostic Modalities

One of the fastest developing areas within medicine, both in clinical settings and in research and development, is medical imaging. [50] Medical imaging can be defined as a set of techniques that, in most of the cases, provide images of the internal parts of the body in a noninvasive manner. The term ‘‘noninvasive’’ means here that imaging modalities do not penetrate the skin physically. Medical imaging covers various imaging modalities, including ultrasound (US), x-ray-based methods (e.g. radiography and computed tomography (CT)), magnetic resonance (MR), nuclear medicine (e.g. positron emission tomography (PET) and single photon emission computed tomography (SPECT)), and other methods in optical imaging [22]

Medical imaging plays an important role in patients' care and is continuously being used in managing health and disease [23] For example, it is used in prevention, early detection of disease, choosing an optimal treatment, during surgical interventions, monitoring of treatment effects, etc. [24] During surgical interventions, the imaging modality has to be readily available and preferably provide images in real-time for optimal guidance. [25]

To allow further development of image-guided therapeutic interventions and diagnostic imaging techniques and systems, phantoms that simulate human or animal tissue are needed. [25]

1.1. Conventional X-ray

X-ray tubes generate X-rays based on the classical Röntgen mechanism. [26] which is the common source for medical, dental and routine industrial uses. Electrons emitted from a heated tungsten filament (cathode) are accelerated to 20–100 keV and electrostatically focused onto a metal anode. The electrons lose energy as they interact with the anode and some of this energy is emitted in the form of X-rays. The source size is typically a few mm, but that size can be reduced to a few μm with a smaller electron filament and more sophisticated focusing, the emitted X-rays are both characteristic(fluorescent X-rays from the target material) with discontinuously defined energies and bremsstrahlung X-rays with a continuous energy spectrum. Although this conventional source provides a large field-of-view usually required by many medical applications, the source performance is limited by low resolution and absorption-only capability, thus being insensitive to subtle changes in electron density in biological tissues. [27]

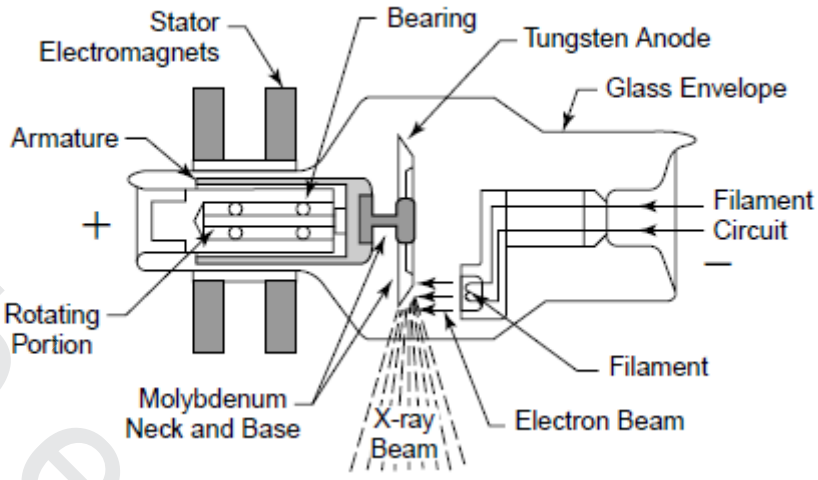

Figure (1): Simplified x-ray tube with a rotating anode and a heated filament. [28]

1.1.1. X-ray Detector

They are devices used to measure the spatial distribution, spectrum or other properties of X-rays, Imaging detectors for radiography were originally photographic plates and photographic film, Photographic film is an old-fashioned X-ray detector still used in medicine and dentistry. It is relatively inexpensive and provides a permanent record with a spatial resolution typically ranging within 10–100 μm. Photographic film is developed using wet chemistry in a film-developing apparatus. Image plates are similar to film in resolution and sensitivity, but they are reusable. Image intensifiers use a phosphor screen to convert X-rays to visible light, followed by a photocathode that converts visible light to electrons. Image intensifiers possess excellent time resolution [28]

1.2. Computed Tomography

The basic principle of computed tomography includes the fact that the internal structure of any three-dimensional subject can be reconstructed from many different projections or views of that subject. This fact necessitates the collection of large amounts of specific data to reconstruct an accurate picture of the original structure. [29]

Historically, the early scanner configurations were characterized as successive generations of scanner geometry (Fig.2). By 1990 rotating fan beam systems, utilizing slip-ring technology to allow continuous rotation of x-ray tube and detector, had reduced acquisition time to about 1 second, with reconstruction computations requiring several seconds per slice. [30]

The time required to scan a patient volume of interest often was longer than a single breath-hold, and scan range was limited by x-ray tube heat load to 10 to 30 cm. By translating the patient table continuously through the rotating gantry, termed helical or spiral scanning, volume coverage and scan speed were further increased, with fundamental rate limitations being x-ray. [30]

Tube output and mechanical rotation rate, Image reconstruction techniques were developed to interpolate 2D planes from the 3D datasets that were acquired in helical

mode. In the late 1990s, the obstacles encountered by early helical scanners were overcome by multidetector row technology, using multiple sets of detector rows to utilize more of the x-ray tube output and acquire measurements at multiple section levels in parallel. (30)

Reconstruction under these conditions is inherently 3D, so more complex algorithms must be used. Benefiting from substantial improvements in computing power, the rapid increases in CT performance appear to be sustainable into the new century, with development of flat panel detectors, faster electronics, and cone-beam geometry reconstruction algorithms. (30)

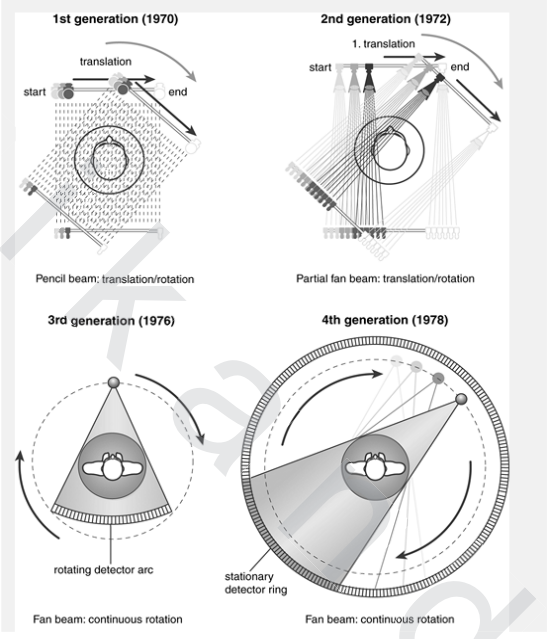

Figure (2): Computed tomography generations. (30)

1.2.1. Computed tomography image formation

1.2.1.1. X-Ray Signals

X-ray imaging consists of the generation of x-rays, transmission of those x-rays through material objects, and the detection of the beam energy that exits the object. The attenuation of x-rays within an object is governed by interactions on the atomic scale, in which each molecule in the object has some cross section for interacting with each x-ray.(30)

Because of this interaction, the x-ray flux decreases on average by a certain percentage for each unit distance traveled through the object. Thus, if a 60 keV x-ray travels through 1 mm of water, on average it will survive 97.4% of the time. For 2 mm of water, the survival probabilities multiply for a 95% rate. (30)

The transmission probability is thus an exponentially decreasing function of the total amount and type of material present, represented by Lambert-Beer equation: (30)

Eq. 1 $$S = I \exp\left(-\sum_i \mu_i t_i\right)$$

Where S is the number of surviving signal quanta, I is the number of incident quanta, the subscript i indicates different materials that are compose the sample, μi is the linear attenuation coefficient for each material and μi is the amount (thickness) of that material present. (30)

In projection x-ray imaging, the image consists of the relative changes in the signal S across a viewing area. For a 70-kg person, with an abdomen roughly equivalent to 20-cm thickness of water, the survival probability for a single quantum would be about 2%. The presence of an additional 2 mm of abnormal structure would change this survival probability to 1.98% (only a 1% difference). Given this small change in the midst of many overlapping body structures, it is clear that projection radiography is limited in its ability to demonstrate anatomic details. (30)

In CT imaging, measurements of S are made from multiple projections, and from these measurements μi is computed for direct display. This technique results in much higher relative contrast between adjacent structures. For example, a 2-mm calcified nodule may have a 200% difference in attenuation coefficient compared with surrounding tissue, and hence be much more conspicuous than on a projection radiograph. (30)

For the viewing of images, projection x-rays are presented as a brightness that is proportional to the changes of the transmitted signal S in Eq. 2. In CT, the image attenuation map is presented in units that are relative to the attenuation coefficient of water μ_{water}, expressed as Hounsfield units (HU) while μi is the attenuation coefficient of the measured material. (30)

Eq. 2 $$HU_i \equiv 1{,}000\,\frac{\mu_i - \mu_{\text{water}}}{\mu_{\text{water}}}$$ (30)

1.2.2. Computed Hounsfield Units Numbers

The baseline for HU numbers in CT is water, which is assigned the value of 0. Scanners are calibrated so that water is always "0." Therefore dense, cortical bone has a value of +1000, or up to +3000 in some modern scanners. Air producing the least amount of attenuation has the value of -1000. Between these two extremes are tissues and substances that possess different HU numbers in CT according to their attenuation. Different shades of gray are assigned specific HU numbers in CT to create the displayed image. (29-30)

1.2.3. Source and Detector Collimation

In CT, collection of this data requires very close collimation to limit the radiation beam to the area of interest. The x-ray beam is actually collimated before and after it passes through the patient's body. The source collimator is located very close to the x-ray tube, and a detector collimator is located close to each detector in the detector array. The actual thickness of the tomographic slice is controlled by the source collimator and ranges

from 0.5 to several millimeters. The detector collimators limit the amount of scatter radiation picked up by the detectors. Because each section is very thin and tightly collimated, little secondary and scatter radiation escapes to neighboring tissue. [29]

1.2.4. Volume Element (Voxel)

After many transmissions of x-ray data the reconstructed anatomy in the form of a digital image appears to be composed of a large number of tiny, elongated blocks. Each of the tiny blocks represents a volume of tissue as defined by the opening in the source collimator. In CT language, each block is termed a volume element, which is shortened to voxel. Voxels are three-dimensional tissue elements that have height, width, and depth. The depth of a voxel is determined by the slice thickness as selected by the scanner operator. [29]

Any CT slice, such as in Figure 3, is composed of a large number of voxels representing various degrees of attenuation, depending on the density of the tissue represented. [29]

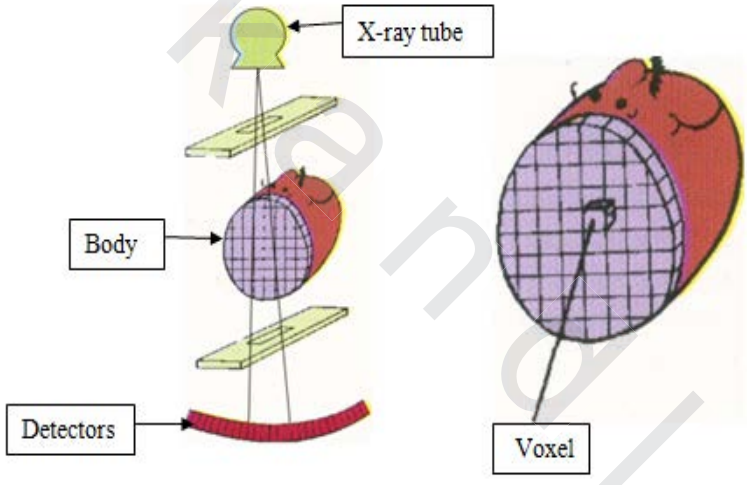

Figure (3): Composition of CT slice [29]

1.2.5. Attenuation (Differential Absorption) of Each Voxel

Each voxel in the tissue slice is assigned a number proportional to the degree of x-ray attenuation of that entire chunk of tissue or voxel. In computed tomography these data from differential absorption of tissue by voxel elements are collected and processed by the processing unit of the computer. [29]

1.2.6. Converting Three-Dimensional Voxels to Two-Dimensional Pixels

Once the degree of attenuation of each voxel is determined, the three-dimensional tissue slice is projected on the computer monitor as a two-dimensional image with only height and width. This two-dimensional image is termed the display matrix and is composed of tiny picture elements termed pixels. Each voxel of tissue is then represented on the television screen as a pixel. The number of individual elements or pixels comprising the display matrix is determined by the manufacturer, with higher resolution monitors having a greater matrix size (i.e., more and smaller pixels) figure 3 . [29]

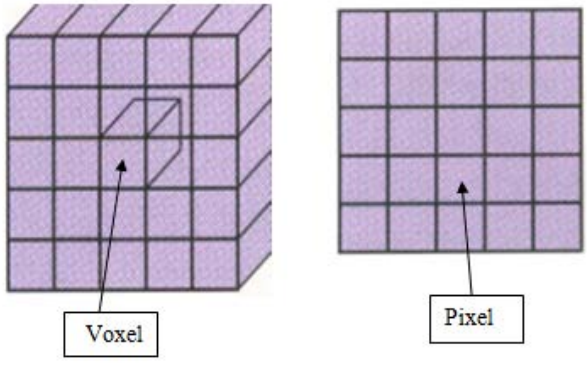

Figure (4): Voxel presented on the monitor screen as a pixel. [29]

1.3. Ultrasound

Ultrasound is cyclic sound pressure with a frequency greater than the upper limit of human hearing. Although this limit varies from person to person it is approximately 20 kilohertz (20.000 hertz) in healthy, young adults and thus, 20 (kHz) serves as a useful lower limit in describing ultrasound. The range normally used in medical field is from 3-15 MHz. [31]

Ultrasound waves begin with the transducer, typically a piezoelectric material, where an electrical pulse is converted to an ultrasound pulse. The ultrasound pulse is comprised of a modulated sinusoidal carrier signal, typically at the resonant frequency of the transducer. As the ultrasound pulse travels through tissue, interactions with boundaries between tissues of different acoustic impedance will cause some of the energy of the pulse to reflect back towards the transducer. Due to the natural characteristics of piezoelectrics, the reflected ultrasound energy that returns to the transducer is reconverted back into an electrical signal. Depending on the speed at which sound travels through the tissue, the returning echo will arrive at the transducer after some time delay (td), which is proportional to the depth of the scattering boundary: [32]

$$t_d = \frac{2 \cdot depth}{c_{sound}}$$

Eq.3

Where C sound is the speed of sound within the tissue of interest, Ultrasound travels through a medium as a mechanical and longitudinal vibration of the medium's particles, where the particles of the medium can be thought as connected by springs, effectively making the medium elastic. The propagation speed of the ultrasound wave (co) will be dictated by the medium properties, and is determined by. [32]

$$c_o = \sqrt{\frac{\beta}{\rho}}$$

Eq.4

Where β is the bulk modulus and ρ is the density. The speed of sound in water is approximately 1485 m/s, and ranges between 1450 m/s to 1600 m/s depending on the tissue type. The speed of sound (co) can be related to frequency (f) and wavelength (λ) by.[32]

$$c_o = f \cdot \lambda$$

Eq.5

The number of wavelengths in an ultrasound pulse dictates spatial pulse length. An ultrasound imaging pulse is typically three cycles long. [32]

1.3.1. Image Resolution

Resolution refers to the quality of the image produced by the machine. It is the ability to differentiate the anatomical and pathological areas of interest with greater detail. While there are several factors that contribute to the overall image quality, we will limit our discussion to axial, lateral, temporal, and contrast resolution. [33]

1.3.2. Axial Resolution

Axial resolution is the ability to differentiate two closely spaced echoes that lie in a plane parallel to the direction of sound wave propagation. The ability to distinguish these echoes in greater number improves the resolution. If we consider the dpi (dots per inch) setting commonly available on a computer printer, the greater the dpi setting provides us with greater image resolution and a higher quality image. [33]

There are several factors that contribute to the quality of the axial resolution; however, the rate-limiting step under control by the operator is the ultrasound beam and transducer frequency. In general, the higher the transducer frequency the better the resultant image quality (Figure5). [33]

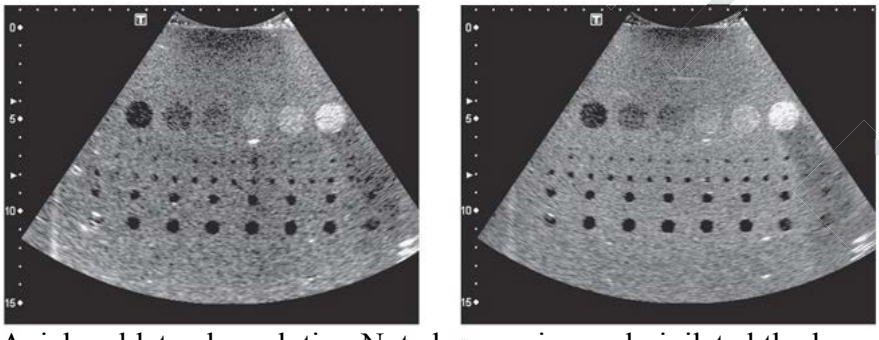

Figure (5): Axial and lateral resolution Note how grainy and pixilated the lower frequency (1.9 MHz) image is (A) compared to the smoother characteristics of the higher resolution (5.0 MHz) image (B). Both images were obtained using a multipurpose phantom. [33]

1.3.3. Lateral Resolution

Lateral resolution is the ability to differentiate two closely spaced echoes that are positioned perpendicular to the direction of propagation of the ultrasound beam. Generally, lateral resolution will be inferior to axial resolution. The primary equipment control that improves lateral resolution is adjusting the "focal zone" to the area of interest. Some

equipment manufacturers slave the transducer frequency with the "focal zone" and changing the frequency may aid in improving lateral resolution because it adjusts the focal zone to a new segment of the image closer to the area of interest. (33)

Ultrasound beam width contributes to this side-to-side resolution. The width of an average beam emitting from a transducer is approximately 1.5 mm at a focal depth. For transducers incorporating an internal focusing capability, a user selectable adjustment is often available. This adjustment allows the operator to vary the width of the ultrasound beam relative to depth within the image. If this "focal zone" is positioned on the screen adjacent to the area of interest on the ultrasound image, then the ultrasound beam will in theory be the narrowest at this point allowing for improved lateral resolution. (33)

Multiple focal zones may be selected on a single ultrasound image in an attempt to maximize the resolution at specific depths. Since this action requires additional processing time, a slower frame rate will occur and the image will appear to have less of a real-time appearance. Single focal zone capabilities are generally sufficient for most abdominal and cardiac examinations. Multiple focal zones are often of greater value when examining superficial structures when transducer movement is at a minimum and additional signal processing time is of less concern. (33)

1.3.4. Temporal Resolution

Temporal resolution refers to the acquisition rate of a composite frame expressed as frame rate (frames per second) or sometimes expressed as Hz (cycles per second). A frame rate of 15 Hz is required to see structures move in "real time" such as a fetal heart beat or other adult cardiac structures. Adjusting sector width or decreasing line density will have the greatest impact on increasing temporal resolution or frame rate because in both situations the system is scanning fewer lines that require less time. (33)

1.3.5. Contrast Resolution

Contrast resolution refers to the ultrasound system's ability to assign a gray scale value to returning echoes of varying amplitudes. Many diagnostic ultrasound systems today allow an assignment of 256 shades of gray, which facilitates the ability to discriminate between the subtle differences that exist between tissues. A higher contrast (less shades of gray) may be more pleasing to the human eye but may, in fact, contain less diagnostic information. This dynamic range of information (measured in decibels or db) is often a programmable feature on ultrasound systems and may be examination specific. The optimum setting allows a clear differentiation between the area of interest and the surrounding anatomy and typically the more shades of gray the better the contrast resolution. (33)

1.3.6. Modes

1.3.6.1. A Mode

A Mode, or "Amplitude," provided one of the original evaluations of the human body using sound. A Mode ultrasound included an oscilloscope display for returning amplitude information and a traditional picture did not exist. The peak amplitude information on the horizontal axis provided information regarding the strength or "loudness" of the wave, while the vertical axis provided reflector distance information from the transducer (Figure6). [33]

1.3.6.2. B Mode

B Mode, or "Brightness," converts amplitude waveforms into an image allowing better correlation with anatomical structures. Returning signals are assigned a gray-scale pixel based on amplitude. Grayscale scanners display up to 256 shades of grayscale information. These shades of gray allow subtle differences within tissues to be visualized The ultrasound system's ability to divide and display the returning echoes into different shades of gray (64 vs. 256 shades, for instance) corresponds to the ultrasound system's contrast resolution or dynamic range (Figure6). [33]

1.3.6.3. M Mode

M Mode, or "Motion," permits a simultaneous display of the two-dimensional (2-D) B Mode image and a characteristic waveform (Figure6). This waveform depicts the motion or deflection of the tissue relative to the transducer on the vertical axis and represents time or changes in the cardiac cycle on the horizontal axis. M Mode technology can be of value in the emergency and acute care setting during pregnancy examinations and permits measurement and documentation of fetal cardiac activity. It can also be useful to demonstrate timing of events during changes in the cardiac cycle such as identifying right ventricular diastolic collapse secondary to pericardial effusion. Similarly, documentation of lung sliding or similar applications can also be achieved using M-mode. [33]

1.3.6.4. D Mode

D Mode, or "Doppler," is presented in a few different forms. Doppler technology relies on the interpretation the "frequency shift" that exists between the transmitted and received Doppler signal, while the anatomy (blood within the vessel) is moving as it is imaged. [33]

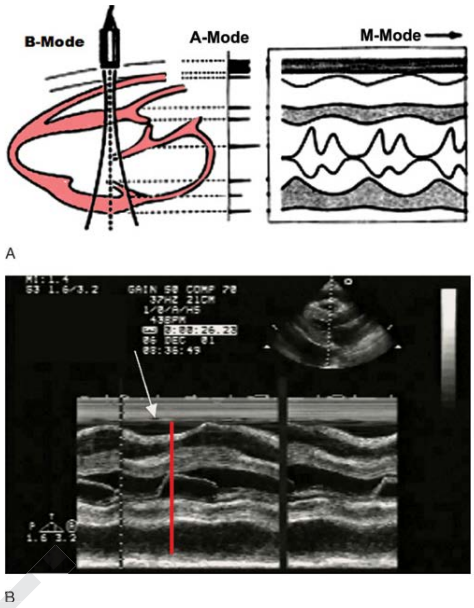

Figure (6): Comparison of modes, the diagram (A) depicts the image display for each of three modes: B-mode, A-mode, and M-mode. The mitral valve is open during ventricular diastole and closed during systole, M-mode ultrasound of pericardial effusion (B). The arrow shows that the RV collapses during early diastole (MV open on right as indicated by red time-line). [33]

1.3.7. Two-Dimensional Imaging

1.3.7.1. Echogenicity

Echogenicity refers to the amplitude or brightness display of the returning echoes. If a structure presents as hyperechoic, it is said to be more echogenic (of increased amplitude) than the surrounding anatomy. Conversely, hypoechoic structures appear less echogenic (of decreased amplitude). Isoechoic information has the same echogenicity as the surrounding structures. Finally, anechoic refers to the absence of echoes. Typically, fluid-filled structures appear anechoic (Figures 7 and 8). [33]

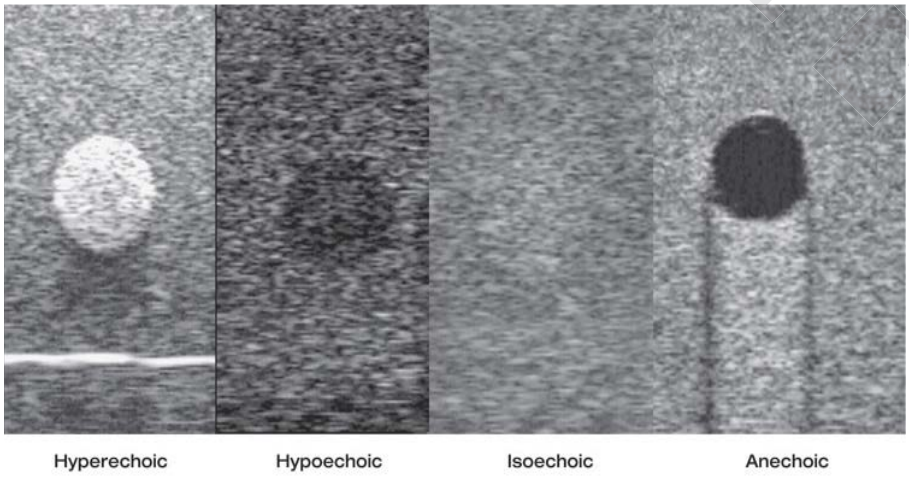

Figure (7): The different US echogenicity

1.3.7.2. Image Artifacts

Unrecognized artifacts are frequently the source of misleading information and misdiagnosis. The ability to recognize and interpret echo information not only includes the anatomical reflections we expect to visualize, but also includes the formation of echoes that appear as a result of image artifacts. Artifacts will be defined as any echo information that does not correspond to the anatomical information as it is positioned and reflected from within the patient. The origin of these artifactual echoes may occur from within the patient, as a result of attenuation or refraction, from an external source, or operator error.[33]

1.3.7.3. Shadowing

Acoustic shadowing is one of the most common and frequently encountered imaging artifacts in diagnostic ultrasound. Shadowing may occur for several different reasons, including anatomical, pathological, or changes undergone by the ultrasound beam. [33]

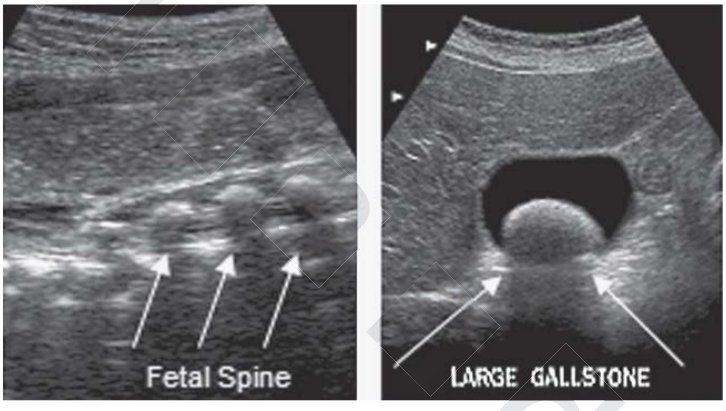

Figure (8): Clean shadowing from attenuation. Bone density objects such as this fetal spine and a large gallstone, generally result in a darker more homogenous ("clean") shadow (arrows). [33]

1.4. Magnetic Resonance Imaging

Magnetic Resonance Imaging (MRI) has become an important noninvasive imaging modality. MRI has found a number of applications in the fields of biology, engineering, and material science. Because it provides unique contrast between soft tissues (which is generally superior to that of CT) and high spatial resolution, MRI has revolutionized diagnostic imaging in medical science. An important advantage of diagnostic MRI as compared to CT is that the former does not use ionizing radiation. [34]

The foundation of the MR phenomenon is the interaction between an external magnetic field and nuclei which have a nonzero magnetic moment. According to the classical theory of electromagnetism, the motion of individual nuclear moments in a static magnetic field B0 is a precession about B0 at an angular frequency w0, known as the Larmor frequency, which is proportional to the strength of the magnetic field. [34]

The nucleus of an atom exhibits magnetic characteristics which are influenced by the spin and charge distributions. When the total number of protons is not equal to the number of neutrons in a nucleus, there is a magnetic moment created due to the nuclear spin.

Hydrogen has a large magnetic moment and is abundant throughout the human body, primarily as part of water molecules, and thus is the principle element for magnetic resonance imaging. (34)

Magnetic resonance imaging begins with the alignment of paramagnetic nuclei within a high magnetic field, usually 1.5T or 3T in strength. Protons in this field will align with the magnetic field in either a parallel or anti-parallel orientation, where the sum of their magnetic moments will produce a net magnetic moment in the direction of the magnetic field. In addition, the magnetic field will cause the spinning protons to process at an angular frequency (ωo) that is proportional to the magnetic field strength (Bo). This relationship is described by the Larmor equation (34)

$$\omega_o = \gamma \cdot B_o$$

Eq.6

Where Y is the gyromagnetic ratio, a constant for each element, For hydrogen, Y is equal to 42.58 MHz/T. (34)

The equilibrium of the net magnetic moment can be disturbed by application of a radiofrequency pulse tuned to the Larmor frequency, whose magnetic component is termed *B1*. The displacement of the longitudinal magnetization vector to generate transverse magnetization is described by the flip angle. A 90-degree flip angle will place the entire longitudinal magnetization in the transverse plane. The time it takes for the return of the longitudinal magnetization back to equilibrium is the T1 relaxation time, or the spin-lattice relaxation time, since the excited protons release their energy to the tissue (molecular lattice). (34)

The radiofrequency pulse will also align all the protons to the same phase. Local micromagnetic inhomogeneities due to the individual magnetic fields of each proton can cause a spin-spin interaction, whereby the aligned protons will precess at different frequencies. The time it takes for transverse magnetization to decay to zero is due to the loss of phase coherence and is termed the T2 relaxation time, or the spin-spin relaxation time. (34)

T1 is typically longer than T2. The spins may also get out of phase due to the externally applied magnetic field. There will always be slight variations in the homogeneity of the applied magnetic field which will cause protons in different locations to precess differently due to slightly different magnetic field strengths. (34)

The decay of transverse magnetization described by both spin-spin interactions and the external magnetic field is called T2*. T2* will always be less than T2. The time interval between applications of radiofrequency pulses is called the repetition time, or TR. Many pulses will be applied in order to form an MR image. (34)

For MR imaging, the radiofrequency pulse used to tip the net magnetic moment is applied in the presence of a magnetic field gradient (Gz), and is modulated by a frequency envelope such as a sinc or Gaussian waveform. The magnetic field gradient will vary the magnetic field strength along an axis, thus causing only the protons with resonant frequencies within the frequency bandwidth of the radiofrequency pulse to be excited. (34)

These excited protons will emit a signal which is called the free induction decay (FID). One problem is that the FID dephases very rapidly and may disappear before it can be measured. Time is required to apply spatial encoding gradients to spatially encode the signal. Thus, the FID is intentionally dephased and rephrased (or recalled) at a later time, the echo time (TE). (34)

The use of Gz allows for slice selection in MR imaging, and the slice thickness can be controlled with either the gradient strength or by altering the radiofrequency pulse bandwidth. Once a slice has been localized, the MR signal must be localized in two other perpendicular directions to create an image of the slice; this is spatial encoding. After application of Gz, all the protons within a slice are processing at the same frequency. (34)

Applying another gradient, the phase encoding gradient (Gy) in plane of this slice for some time will induce a phase shift, whereby some protons will experience a higher net magnetic field and will process faster, and some will experience a lower magnetic field and process slower. Once the Gy gradient is turned off, all the protons will experience the same field strength and precess at the same frequency, however there will be a phase shift along the y-axis. This is phase encoding. (34)

Applying another gradient perpendicular to Gz and Gy (Gx) during the reception of the recalled signal alters the frequency along this axis (frequency encoding). Applying Gx during the reception of the signal (readout) provides positional information along that axis, and fills a line in 'k-space' corresponding to a specific Gy. This happens for every TR interval, and for every TR a different Gy strength is applied to induce a different phase shift value. In summary, a unique frequency will represent an x-position while a unique phase will represent a y-position in k-space. K-space is the space in which the recorded data is written, and a Fourier transform is performed on k-space to get from frequency information to spatial information. (34)

In order to emphasize the differences in spin characteristics within tissue, a pulse sequence is used to make the emitted signals dependent on T1, T2, T2*, or spin density. A pulse sequence is a sequence of repeatedly applied radiofrequency pulses that occur during an MR study. If the pulse sequence emphasizes T1 characteristics, we would say that it is T1-weighted. The same applies for T2, T2*, and spin density. (34)

1.4.1. T1-Weighted Imaging

T1-weighted imaging implies contrast is produced primarily from different T1 characteristics in tissue, and where T2 contributions are considered negligible. One method of achieving T1-weighted imaging is by using a spoiled gradient recalled echo pulse sequence (SPGR). A characteristic of gradient recalled echo sequences is there is residual transverse magnetization at the end of each TR, which will be affected by the next few RF pulse cycles until it reaches steady state. (35)

The spoiled gradient recalled echo pulse sequence eliminates (‚spoils') the residual transverse magnetization, thereby reducing the T2* weighting and increasing the T1 weighting. Signals measured using an SPGR sequence can be converted to T1 using the SPGR equation, (35)

$$M_{xy} = \frac{M_o \cdot (1 - e^{\frac{-TR}{T1}}) \cdot sin\theta}{(1 - cos\theta \cdot e^{\frac{-TR}{T1}})}$$

Eq.7

Where M_{xy} is the measured signal intensity, Mo is the equilibrium longitudinal magnetization, TR is the repetition time, and θ is the flip angle. Mo can be determined with a known T1, such as the native T1 (T10), which is the T1 pre-contrast injection. The SPGR equation can also be re-written to solve for T1. [35]

$$T1 = \frac{-TR}{ln\left(\frac{M_{xy} - sin\theta \cdot M_o}{M_{xy} \cdot cos\theta - M_o \cdot sin\theta}\right)}$$

Eq.8

1.4.2. Measuring T1

Measuring native T1 (T10) can be quite challenging. An inversion recovery spin echo (IR-SE) pulse sequence can be used to make a reliable assessment of T1, where several measurements are made using a series of different inversion times (TI), and the resultant corresponding signal intensities are fitted to the equation[35]

$$SI(TI) = abs\left(SI_{inf} \cdot (1 - k) \cdot e^{\frac{TI}{T1}}\right)$$

Eq.9

Where SI (TI) indicates the signal intensity at a specific TI, SI inf is the signal intensity from the spin system in thermal equilibrium, and k corresponds to the cosine of excitation angle of the inversion pulse. [36] It has been shown that an inversion recovery fast spin echo (IR-FSE) can also be used with good efficiency to calculate the native T1 relaxation time. [37] Several other methods have been investigated for quickly measuring T1, such as Look-Locker and variable flip angle methods. [37-38]

2. Phantoms

A phantom in the setting of radiology research may be defined as an imitation or representation of an organ, body part, physiologic process or pathologic condition. Investigations employing phantoms are commonly performed in radiology research, in some instances a phantom study may serve as a pilot study prior to an investigation in living persons. [39]

Phantoms that simulate human or animal tissue are needed to allow further development of image-guided therapeutic interventions and diagnostic imaging techniques and systems. [40]

Most of the commercially available phantoms are adapted for a broad market and are designed for particular applications, those phantoms are rather expensive and they are not meant to be modified or custom-fitted by the users [39]

To customize design and fabrication of the phantoms, and to overcome the abovementioned disadvantages, various studies focus on development of techniques and ingredients to prepare tissue-mimicking materials [41]

2.1. Soft tissue mimicking materials

A multitude of techniques and tissue-mimicking materials have been proposed to prepare phantoms. The most often-used bulk matrix materials for mimicking soft tissue are based on: aqueous suspensions, agarose, gelatin, magnesium silicate, oil gel, polyacrylamide gel, polyurethane resin, polyvinyl alcohol (PVA), polyester resin, epoxy resin, polysaccharide gels TX-150 and TX-151, polyacrylamide, and Room-Temperature-Vulcanizing (RTV) silicone [42]

Aqueous suspensions are the simplest tissue substitutes, in which water is used as a substitute of a tissue. Agarose- and gelatin-based tissue substitutes (also called hydrogels) are the most widely used alternatives of soft tissue, the reasons for that are: well-characterized performance, ease of fabrication, and flexibility provided by the process that allows achieving a range of acoustic properties. [39] Reported main disadvantages of using both agarose- and gelatin-based phantoms are their lack of longevity (often limited to less than one month because of microbial invasion), and delicate structure that can easily be damaged, inclusion of biochemically toxic species prevents bacterial growth in these two tissue-mimicking materials. [43]

Oil gel-based substitutes consist of a propylene glycol, a gelatinizer, and 10 mm polymethyl methacrylate microspheres, their main advantages are: resistance to bacterial infection, and linear increase of speed of sound and attenuation with the proportion of propylene glycerol. Ethylene glycol-based oil gels, however, are not perfect substitutes of soft tissue for multimodal phantoms, because of their US characteristics; i.e. speed of sound and density is too high, and attenuation is too low. Polyurethane, polyester and epoxy resins have been reported to have good characteristics for mimicking soft tissue, including low Young's modulus, elastic recovery and immunity to bacterial infection [43]

The standardization of the polyurethane gel-based phantoms production, however, is problematic due to complex molecular design of the gels. PVA-based tissue substitutes (also referred as cryogels) have indefinite longevity, are low cost, and require a smaller amount of ingredients than the agarose- and gelatin-based tissue substitutes. [44]

Preparation of the PVA-based phantoms requires multiple 12-h freeze-thaw cycles and precise control of the temperature. Polysaccharide gels are used to prepare an inexpensive, conveniently moldable, and temporally stable tissue equivalent, using polysaccharide gels requires controlling gelling time by means of temperature and the ratio of the polysaccharide gel to water. Often encountered problem when making this gel mixture is incorporation of bubbles, which is a problem for US imaging. Polyacrylamide gel-based tissue substitutes are made by polymerization of the acrylamide monomer. [45]

Since polyacrylamide is highly toxic, special precautions during its preparations are needed. The advantage of using RTV silicone is that the phantoms can be quickly produced. [46] Besides, RTV silicone provides a soft rubber texture similar to that of stiff tissue. The major two shortcomings of using this material are cost and hardening time. Next to choosing bulk matrix materials, scattering particles need to be selected for optical phantoms. Often, this selection is made separately from the choice of the matrix structure. The four most common choices of scattering agents are: lipid microparticles, polymer microparticles, white metal oxide powders (including TiO2 and Al2O3 powders), and quartz glass microspheres. [47]

Lipid microparticles of 10 to 500 nm are biologically analogous to bilipid membranes of cells and organelles, which are believed to cause scattering in tissue. Commercially available lipid-based scatterers are milk, fat/oil/lipid and Intralipid/ Nultralipid, polymer microspheres of 50 to 100 mm are produced in regular sizes, which means that repeatability and predictions of spectra are good due to well-controlled size and index of refraction ide availability of TiO2 powder, 20 to 70 nm, makes titanium dioxide one of the most commonly used scatterers. [48]

The key drawback of the TiO2 powder is that it settles when not stirred, which is a problem when fabricating aqueous suspensions. Therefore, TiO2 powders should be used for manufacturing gelatin- or agarose-based, RTV, and resin phantoms. The use of quartz glass microspheres (250 nm) is less established [49]

2.2. Magnesium silicate–based tissue substitutes

Magnesium silicate is an inorganic substance with a structural form that varies with applied stress .Soft tissue-mimicking materials were created by mixing magnesium silicate with tetra sodium pyrophosphate (an electrolyte needed for the hardening of the gel), n-propanol (to control the speed of sound), water and either graphite or talcum powder(as scattering agents to vary attenuation). [50]

Magnesium silicate–based tissue substitutes have the advantage of temperature stability (stable from 0 to 100 C), resistance to microbial invasion and the ability to reform after needle biopsy procedures .[50]

Open cell foam–based tissue substitutes A soft tissue substitute was developed based on open cell foam, which is composed of polyurethane foam and a salt (NaCl) water solution. [51]

An advantage to this process is that localized zones mimicking tissue pathologies or variations can be created within the material by removing regions of foam before preparation, therefore allowing for the creation of simple inhomogeneous phantoms. [51]

2.3. Soft tissue phantoms

2.3.1. Brain phantoms

Various soft tissue substitute preparation techniques can be used to create brain phantoms. One group used an agarose- based technique originally developed for prostate phantoms to create a brain phantom that was used for the evaluation of anon invasive focal brain surgery [52]

Another group used a PVA fabrication process, initially developed for soft tissue, to make an anthropomorphic brain phantom, usinga3-D magnetic resonance image (MRI) to create the phantom mold [53]

2.3.2. Liver phantoms

Liver tissue substitutes have been created using several techniques described for general soft tissue. Homogeneous liver phantoms have been made from gelatin and graphite, similar to the [54]

2.3.3. Prostate phantoms

Materials that simultaneously mimic soft tissue in vivo for magnetic resonance imaging (MRI), ultrasound (US) and computed tomography (CT) for use in a prostate phantom have been developed. Prostate and muscle mimicking materials contain water, agarose, lipid particles, protein, Cu++, EDTA, glass beads, and thimerosal ~preservative!. Fat was mimicked with safflower oil suffusing a random mesh network of polyurethane.[55]

2.3.4. Multi-organ phantoms

Phantoms have been developed that mimic complete organ systems rather than individual tissues or organs. [56] Developed a torso section using water-alcohol–based gelatin with n-propanol and various test objects to mimic the kidneys, liver, tumors, cysts and bones. [57]

Rowan and Pederson created a multi-organ phantom using latex to mimic skin, agar and graphite to mimic organs and leaking silicon tubes to simulate internal bleeding as a training tool for the diagnosis of internal trauma. [57]

3. Contrast Imaging

Contrast-enhanced imaging has been developed as a tool to study tumour vasculature. The abnormal pathophysiology and microvascular structure gives rise to temporal and spatial variations in signal enhancement that differ from normal surrounding tissue, which can be used to provide information on tumour characteristics. Some of the physiological characteristics of interest include blood flow, blood velocity, vessel permeability, and microvascular vessel density. Some studies have investigated the prognostic value of these parameters and their ability to monitor response to a therapy based on their changes, contrast-enhanced imaging studies typically begin with the intravenous administration of a contrast agent bolus through a peripheral vein, Bolus injection methodology is of considerable importance, and must be done in a consistent manner. [58]

A contrast agent is considered intravascular or extravascular. Intravascular contrast agents are assumed to never leave the vascular system due to their large size in comparison to the spaces between vessel wall endothelial cells. Extravascular contrast agents, by comparison, are small enough such that they traverse vessel walls through the endothelial cell junctions into the space outside the vasculature. This process is often mediated by diffusion. [59]

3.1. Iodinated Contrast Media

Current radiological imaging uses either electromagnetic radiation (X-rays or radiowaves) or ultrasound. X-rays have a frequency and photon energy several powers higher than visible light and can penetrate the body. The radiation which emerges from the body is detected either by analogue radiological film or by a variety of digital media. The radiowaves used in magnetic resonance imaging have a frequency and photon energy several powers lower than visible light. (60)

The radiowaves cause deflection of protons in the body which have aligned in the magnetic field in the scanner and as the protons relax back to their resting position, they emit radiowaves which are used to generate the image. Ultrasound imaging uses sound (pressure) waves several powers higher than audible sound which are reflected back from tissue interfaces in the body to generate the image. Contrast media may be used with all of these imaging techniques to enhance the differences seen between the body tissues on the images. (60)

Contrast media alter the response of the tissues to the applied electromagnetic or ultrasound energy by a variety of mechanisms. The ideal contrast medium would achieve a very high concentration in the tissues without producing any adverse effects. Unfortunately, so far this has not been possible and all contrast media have adverse effects.(60)

3.2. Radiographic Contrast Media

Radiographic contrast media are divided into positive and negative contrast agents. The positive contrast media attenuate X-rays more than do the body soft tissues and can be divided into water soluble iodine agents and non water soluble barium agents. Negative contrast media attenuate X-rays less than do the body soft tissues. (60)

3.3. Iodine Agents

Water soluble iodinated contrast agents which diffuse throughout the extracellular space are principally used for angiography, during computed tomography (CT) and conventional radiography They can also be administered directly into the body cavities, for example the gastrointestinal tract and urinary tract. All of these contrast media are based on a benzene ring to which three iodine atoms are attached. A monomer contains one tri-iodinated benzene ring and a dimer contains two tri-iodinated benzene rings. Iodinated contrast media can be divided into two groups, ionic and nonionic based on their water solubility. (60)

The water in the body is polarised unevenly with positive poles around the hydrogen atoms and negative poles around oxygen atoms. Ionic contrast media are water soluble because they dissociate into negative and positive ions which attract the negative and positive poles of the water molecules. Nonionic contrast media do not dissociate and are rendered water soluble by their polar OH groups. Electrical poles in the contrast medium OH groups are attracted to the electrical poles in the water molecules. (60)

The osmolality of contrast media affects the incidence of side-effects. The early contrast media had very high osmolality's (1500–2000 mosm per kg) and subsequently

agents of lower osmolality have been developed. Contrast media may be divided into high-, low- and iso-osmolar agents. An indication of the osmolality of an agent is given by the contrast medium ratio which is derived by dividing the number of iodine atoms in solution by the number of particles in solution: [60]

$$Contrast\ medium\ Ratio = \frac{Number\ of\ iodine\ atoms}{Number\ of\ particles\ in\ solution}$$

Eq.10

The higher osmolality agents have more particles per iodine atom and therefore have lower ratios. Thus the ionic monomers have a ratio of 1.5 (three iodine atoms per two particles in solution), the nonionic monomers and the ionic dimers have a ratio of 3 (three iodine atoms per particle in solution) and the nonionic dimers have a ratio of 6 (six iodine atoms per particle in solution) (Fig9). [60]

The nonionic dimers are iso-osmolar with blood (300 mosm per kg) at all concentrations. Using these properties four different classes of iodinated contrast may be defined (Fig.9): 1. Ionic monomeric contrast media (high-osmolar contrast media, HOCM), e.g. amidotrizoate, iothalamate, ioxithalamate2. Ionic dimeric contrast media (low-osmolar contrast media, LOCM), e.g. ioxaglate3. Nonionic monomeric contrast media (low-osmolar contrast media, LOCM), e.g. iohexol, iopentol, ioxitol, iomeprol, ioversol, iopromide, iobitridol, iopamidol, 4. Nonionic dimeric contrast media (iso-osmolar contrast media, IOCM), e.g. iotrolan, iodixanol. [60]

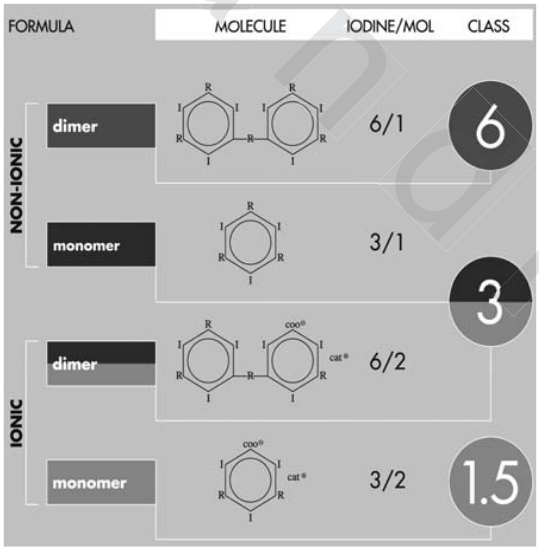

Figure (9): Classification of iodinated contrast media [60]

3.4. Contrast in X-ray Imaging

Since its discovery, medical radiology has been one of the most popular applications of X-rays. In most cases, the contrast in radiology images is based on the different X-ray absorption of the different parts of a specimen. However, absorption is actually limited for X-rays. Weak absorption means small absorption differences among the tested materials, resulting in limited contrast thus low image quality. When an X-ray beam traverses a matter both absorption and deflection of photons occur. [61]

The intensity reduction caused by these processes defines the degree of X-ray attenuation, which obeys the Beer-Lambert law: $I = I0e^{-\mu x}$, where I is the transmitted X-ray intensity, $I0$ is the incident intensity, and x is the thickness of the matter. The mass attenuation coefficient (μ) is the sum of the three interactions between X-ray photons and traversed matter in the proper energy range for diagnostic imaging by the unit of cm2/g: coherent scattering (ω), the photoelectron effect (τ), and Compton scattering (δ): $\mu = \omega + \tau + \delta$. Coherent scattering ($\omega$) produces scattered radiation and noise on X-ray films, but its effect on X-ray image quality is minor. [62]

But the photoelectron effect (τ) is considerable when the X-ray photon energy is greater or almost the same as the electronic binding energy. The greater the photon energy, the less X-ray absorption will occur in this process, thus τ is inversely proportional to the third power of photon energy E: $\tau \propto 1/E3$. Compton scattering is responsible for almost all scattered radiation, which both increases noise and decreases contrast. [62]

The quantity of Compton scattering diminishes as the X-ray photon energy increases, so that high energy photons are more likely to pass through the human body than low-energy photons. As a result, the radiation exposure to patients is lower with high energy X-rays than that with low-energy X-rays. Since very low energy X-rays will produce unacceptable radiation doses to patients and high-energy X-rays diminish the inherent contrast, X-ray energies used in current medical imaging procedures represent a compromise between optimal image quality and patient radiation dose. [62]

The inherent contrast between bone and other tissues is large enough for clinical use in the low to middle X-ray energy range. The mass attenuation coefficient increases with atomic number increase of elements in periodic table, and decrease with energy increase of X-rays. [62]

Many theoretical and experimental studies have also shown that higher atomic number elements demonstrate superior X-ray attenuation ability at normal or even higher operating tube voltages due to the higher K-edges of heavy elements. The K-edges of heavy elements lies within the diagnostic X-ray spectrum as such an abrupt increase in attenuation at discrete energies near the K edge is observed. Thus a contrast media based on elements with higher atomic number will be more advantageous in terms of intrinsic contrast, lower dose requirement and lower radiation exposure to patients. [63]

To increase X-ray contrast, long-time exposure and relatively high doses also can be attempted, which are not advisable for medical application though. Instead, the contrast can be increased by injecting a high-contrast material into the imaged specimen. . [63]

3.4.1. Absorption-Contrast X-ray Imaging

Absorption-contrast X-ray imaging visualizes the X-ray attenuation variation within the volume of a given sample, whereas phase-contrast X-ray imaging visualizes spatial variations in X-ray refractive indices. Absorption-based X-ray imaging is an important paradigm of X-ray radiography, and it enables a vast domain of applications, such as imaging of bone fractures, coronary arteries and the diagnosis of breast cancer. [64] All these applications utilize the high penetrating nature of X-rays. In absorption contrast, the shadow cast by the object is softened at the edges by a mechanism known as penumbral blurring (e.g., source-size blurring). [65]

The detrimental effects of such blurring can be reduced by making the object-to-detector distance or the source size as small as practicable. The former used in conventional radiography works by placing the imaging detector close to the sample to be imaged. This simple and powerful technique makes contact-mode absorption-contrast radiography insensitive to the refractive effects of a typical sample. Different from synchrotron sources, in conventional medical X-ray imaging, the source size is too large for phase contrast and there is a limitation in increasing the distance between the sample and the detector. . [65]

3.4.2. Phase-Contrast X-ray Imaging

Absorption is not the only type of interaction between X-rays and matters that can enhance the contrast in radiological images. X-ray sources with reasonably high coherence (such as synchrotron) are required for phase-contrast. [66]

Without increasing the X-ray dose, the visibility of the object becomes better with phase contrast. [66] Therefore, the dose can be substantially reduced without jeopardizing the practical image quality. Although phase-contrast radiology depends on the coherence of X-rays from synchrotron sources, real-time studies with high spatial resolution are still difficult. This problem has been tried to be solved using unmonochromatized synchrotron X-rays [67]

The three principal interactions of X-rays with matters are absorption, refraction, and scattering [114] Conventional radiography uses X-ray absorption to achieve contrast, but the samples also refract and scatter photons. The refracted and scattered photons create noises in the image and reduce edge definition. By comparison, diffraction-enhanced imaging (DEI) separately measures refracted X-ray photons from non-refracted ones. Density differences in a sample result in X-ray refraction. In other words, DEI allows observations on the boundaries between tissues having different densities. [67]

Minimal X-ray absorption is possible if high-energy X-rays are used (30–40 keV), thereby resulting in low radiation damage. For example, by a non-destructive DEI technique using synchrotron X-rays, the morphology of live plant seeds is continuously observed for novel insights into the developmental processes of plant anatomy [67]

3.4.3. Iodine-Incorporated Particles

Iodinated derivative is one of the most common contrast enhancers for X-ray imaging. They are small in moelcular weight (approximately 800 to 1,600 Da) and water-soluble. The monomeric ionic agent is diatrizoate, while the monomeric non-ionic agent is iopromide. The dimeric non-ionic compounds are iotrolan and ioxaglate, which exhibit high X-ray absorption due to their high iodine contents, the main difference of these iodinated contrast agents is osmolality: Ionic monomers exhibit high osmolality (1500–2300 mOsm/kg) at clinically relevant concentrations. Non-ionic monomers and ionic dimers are slightly hypertonic (500–800 mOsm/kg). [68]

Non-ionic dimers are isotonic to blood (approximately 300 mOsm/kg). Osmolality affects not only the tolerability of the unencapsulated agents but also their applicability for the entrapment in carriers, recently, osmolality of iodinated contrast media has been

overcome by developing iso-osmolar media and various technologies for encapsulation of Iodinated contrast media. (69)

3.5. MR Contrast Media

Magnetic resonance (MR) imaging contrast agents contain paramagnetic or superparamagnetic metal ions which affect the MR signal properties of the surrounding tissues. They are used to enhance contrast, to characterize lesions and to evaluate perfusion and flow-related abnormalities. They can also provide functional and morphological information. (70)

Contrast agents for magnetic resonance typically alter the relaxation times in order to enhance contrast between different tissue types. The most prevalent type of contrast agents for magnetic resonance are Gd-chelate based. Gadolinium is a Lanthanide element that is paramagnetic in its trivalent state (GdIII). This metal ion has an S ground state structure that couples a large magnetic moment with a long electron spin relaxation time, making it efficient for nuclear spin relaxation when interacting with nuclei. (70)

However, as a free metal ion it is poorly tolerated in vivo as it is toxic. In order to make them clinically viable, GdIII is bound to a ligand. Other properties required of contrast agents along with low toxicity include good water solubility and rapid excretion after administration (70)

Gd-chelate based contrast agents, typically around 500 da in size, are able to freely diffuse from the vasculature into tissue, and vice versa. This movement of the contrast agent between vascular and extra-vascular tissue compartments requires a mathematical model to describe the pharmacokinetics of the contrast agent and its regional distribution, which is governed by parameters such as blood flow, blood volume, the endothelial permeability and surface area, as well as the size of the surrounding extracellular extravascular space (71-72)

Dynamic contrast enhanced magnetic resonance imaging (DCE-MRI) typically involves T1-weighted sequences. For a spoiled gradient recalled echo pulse sequence, a short TR and TE along with a moderate flip angle are used. Low concentrations of Gd-chelate based MR contrast agents will primarily cause a shortening in T1, which is the cause of signal enhancement. This enhancement seen by T1-weighted imaging schemes is due to several factors, such as the native T1 of the tissue, the dose of the contrast agent, the parameters chosen for the given imaging scheme, and the different methods the contrast agent may behave within the physiology, the affected T1 relaxation time can be linearly related to contrast agent concentration (73) by

$$\frac{1}{T1} = \frac{1}{T10} + r_1 \cdot [CA] \quad \text{Eq.11}$$

Where, T10 is the pre-injection T1 of tissue, r1 is the relaxivity [mmol-1s-1], and CA is the contrast agent concentration [mmol]. Relaxivity is dependent on the chemical properties of the contrast agent and is a parameter that describes the agents' ability to increase the relaxation rates of the surrounding water protons. (73)

3.5.1. Paramagnetic Contrast Agents

Paramagnetic contrast agents are mainly positive enhancers which reduce the T1 and T2 relaxation times and increase tissue signal intensity on T1-weighted MR images. (60)

The most widely used paramagnetic contrast agents are non-specific extracellular gadolinium chelates. Their active constituent is gadolinium, a paramagnetic metal in the lanthanide series, which is characterized by a high magnetic moment and a relatively slow electronic relaxation time. Non-specific extracellular gadolinium chelates can be classified by their chemical structure, macrocyclic or linear, and by whether they are ionic or nonionic. They are excreted via the kidneys. (60)

3.5.2. Superparamagnetic Contrast Agents

Superparamagnetic contrast agents include superparamagnetic iron oxides (SPIOs) and ultra-small superparamagnetic iron oxides (USPIOs). Two preparations of SPIOs are available: ferumoxides and ferucarbotran. These particulate agents are composed of an iron oxide core, 3–5 mm in diameter, covered by low molecular weight dextran for ferumoxides and by carbodextran for ferucarbotran. (60)

3.6. Ultrasound Contrast Media

Ultrasound contrast agents produce their effect by increased back-scattering of sound compared to that from blood, other fluids and most tissues. On greyscale images microbubble contrast agents change grey and dark areas to a brighter tone, when the contrast enters in fluid or blood. The spectral Doppler intensity is also increased, with a brighter spectral waveform displayed and a stronger sound heard. Using color Doppler technique, ultrasound contrast agents enhance the frequency or the power intensity giving rise to stronger color encoding. (60)

The level of enhancement of the Doppler signals may be in the order of up to 30 dB. Ultrasound contrast agents can be used to enhance Doppler signals from most main arteries and veins. They may be useful for imaging solid organs, e.g. liver, kidney, breast, prostate and uterus. They can also be used to enhance cavities e.g. bladder, ureters, Fallopian tubes, abscesses. (60)

4. Nanoparticles

The application of nanotechnology to medicine, known as nanomedicine, concerns the use of precisely engineered materials at this length scale to develop novel therapeutic and diagnostic modalities, nanomaterial's have unique physicochemical properties, such as ultra-small size, large surface area to mass ratio, and high reactivity, which are different from bulk materials of the same composition. These properties can be used to overcome some of the limitations found in traditional therapeutic and diagnostic agents. (74)

The use of materials in nanoscale provides unparalleled freedom to modify fundamental properties such as solubility, diffusivity, blood circulation half-life, drug release characteristics, and immunogenicity. In the last two decades, a number of nanoparticle-based therapeutic and diagnostic agents have been developed for the treatment of cancer, diabetes, pain, asthma, allergy, infections, and so on. (124-125) these

nanoscale agents may provide more effective and/or more convenient routes of administration, lower therapeutic toxicity, extend the product life cycle, and ultimately reduce health-care costs. As therapeutic delivery systems, nanoparticles allow targeted delivery and controlled release. (74)

For diagnostic applications, nanoparticles allow detection on the molecular scale: they help identify abnormalities such as fragments of viruses, precancerous cells, and disease markers that cannot be detected with traditional diagnostics. Nanoparticle-based imaging contrast agents have also been shown to improve the sensitivity and specificity of magnetic resonance imaging. (74)

4.1. Types of Nanoparticles

4.1.1. Organic and inorganic nanoparticles

Table (1) Types of Nanoparticles (75)

Organic nanoparticles	Inorganic nanoparticles
Liposomes	Quantum dots
Dendrimers	Polystyrene
Carbon	Magnetic
polymeric micelles	Ceramic
	Metallic nanoparticles

Inorganic nanoparticles have a central core composed of inorganic materials that define their fluorescent, magnetic, electronic and optical properties. (75)

4.1.1.2. Liposomes

Liposomes are phospholipid vesicles (50–100 nm) that have a bilayer membrane structure similar to that of biological membranes and an internal aqueous phase. Liposomes are classified according to size and number of layers into multi-, oligo- or uni-lamellar. (75) Their amphiphilic nature enables liposomes to transport hydrophilic drugs entrapped within their aqueous interior and hydrophobic drugs dissolved into the membrane. (75) Owing to their physicochemical characteristics, liposomes show excellent circulation, penetration and diffusion properties. Moreover, the liposome surface can be modified with ligands and/or polymers to increase drug delivery specificity (75)

4.1.1.3. Dendrimers

Dendrimers are highly branched synthetic polymers (<15 nm) with layered architectures constituted of a central core, an internal region and numerous terminal groups that determine dendrimer characteristics. A dendrimer can be prepared using multiple types of chemistry, the nature of which defines the dendrimer solubility and biological activity. Dendrimers show intrinsic drug properties and are used as tissue-repair scaffolds. Moreover, dendrimers are excellent drug and imaging diagnosis-agent carriers through chemical modification of their multiple terminal groups (76)

4.1.1.4. Carbon nanotubes

Carbon nanotubes belong to the family of fullerenes and are formed of coaxial graphite sheets (<100 nm) rolled up into cylinders. These structures can be obtained either as single- (one graphite sheet) or multi-walled nanotubes (several concentric graphite sheets). They exhibit excellent strength and electrical properties and are efficient heat conductors. Owing to their metallic or semiconductor nature, nanotubes are often used as biosensors. Carbon nanotubes can be rendered water soluble by surface functionalization. Therefore, they are also used as drug carriers and tissue-repair scaffolds [77]

4.1.1.5. Quantum dots

Quantum dots are colloidal fluorescent semiconductor nanocrystals(2–10 nm). The central core of quantum dots consists of combinations of elements from groups II–VI of the periodic system(CdSe, CdTe, CdS, PbSe, ZnS and ZnSe) or III–V (GaAs, GaN, InP and InAs), which are 'overcoated' with a layer of ZnS. Quantum dots are photostable. They show size- and composition-tuneable emission spectra and high quantum yield. They are resistant to photobleaching and show exceptional resistance to photo and chemical degradation. All these characteristics make quantum dots excellent contrast agents for imaging and labels for bioassays. [78]

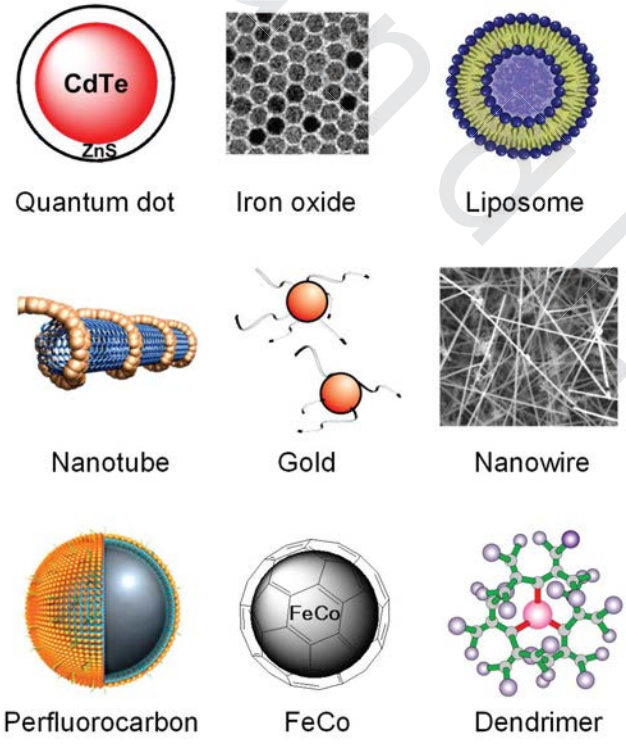

Figure (10): Many nanoparticles have been investigated for biomedical applications targeting cancer. [79]

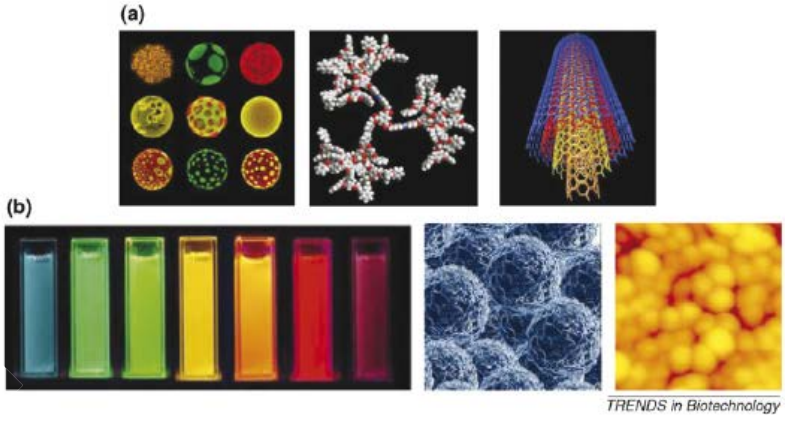

Figure (11): Examples of nanoparticles (a) Organic nanoparticles, from left to right: liposomes, dendrimers and carbon nanotubes. (b) Inorganic nanoparticles. From left to right: quantum dots, magnetic nanoparticles and gold nanoparticles. [79]

4.1.1.6. Metallic nanoparticles

Metallic MNPs, made of iron, cobalt, or nickel, are often overlooked for biological applications due to their chemical instability. Readily forming oxides in the presence of water and oxygen, these metallic MNPs are typically protected by coatings, such as gold or silica, to form a core-shell structure. Despite complex synthesis processes, research continues on these metallic nanoparticles due to the unique advantages some of these MNPs can offer. For example, iron nanoparticles possess relatively high magnetization and are able to maintain superparamagnetism at larger particle sizes compared to their oxide counterparts [80-114]

4.1.1.6.1. Gold Nanoparticles

Gold nanoparticles are one type of metallic nanoparticle; others are Ni, and TiO2 nanoparticles. [130] but it has advantages over other metal nanoparticles due to their biocompatibility and non-cytotoxicity. Nanoparticles are nanometers in size. These are 100 to 1000 times smaller than human cells. The size of gold nanoparticles can be controlled during their synthesis and functionalization with different groups. Gold nanoparticles accumulate in the tumour cells and show optical scattering. . [80]

4.1.1.6.1.1. Characteristics of Gold Nanoparticles

Gold nanoparticles are chemically inert, These have greater biological compatibility, Optical properties like plasmon resonance are exhibited by gold nanoparticles, These exhibit versatility because of their ready functionalization through thiol linkages, Gold nanoparticles provide microscopic probes for the study of the cancer cell, accumulate in the cancerous cell and show the cytotoxic effect i.e. apoptosis or necrosis of the specific cell and cell specific receptor, These have high stability due to the gold-sulphur bonds, Their photo physical properties can be exploited for drug release at remote place. [81-82]

4.1.1.6.1.2. Synthesis of gold nanoparticles

Gold nanoparticles (<50 nm) can be prepared with different geometries, such as nanospheres, nanoshells, nanorods or nanocages. These particles show localized surface plasmon resonant properties, i.e. under the irradiation of light, the conduction electrons are driven by the associated electric field to a collective oscillation at a resonant frequency, thereby absorbing light and emitting photons with the same frequency in all directions. Gold nanoparticles are excellent labels for biosensors because they can be detected by numerous techniques, such as optic absorption, fluorescence and electric conductivity. (83)

4.1.1.6.1.3. Types of Gold Nanoparticles

Gold nanorods, Gold nanoshells, Gold nanocages and Gold nanosphere. (84)

Figure (12): Different types of gold nanoparticles (79)

4.1.1.6.1.4. Gold nanospheres

Gold nanospheres of 2 nm to over 100 nm in diameter can be synthesized by controlled reduction of an aqueous HAuCl4 solution using different reducing agents under varying conditions. The most commonly used reducing agent is citrate, which can produce nearly monodisperse gold nanospheres, the size of the nanospheres can be controlled by varying the citrate/gold ratio. Generally, smaller amount of citrate will yield larger nanospheres. The major limitations of this method are the low yield and the restriction of using water as the solvent. (85)

Many other methods have been investigated for gold nanosphere synthesis such as the use of other reductants or ligands. (86)

There are a number of literature reports on the use of dendrimers as templates or stabilizers for gold nanosphere preparation, biocompatible block copolymers have been employed for the synthesis of sterically stabilized gold nanospheres in aqueous solution, the size and shape of the gold nanospheres could be readily controlled by tuning the synthesis parameters such as the block composition, and the relative/absolute concentrations of the block copolymer and HAuCl4. Growth of gold nanospheres in human cells has also been reported. (87)

Typically, gold nanospheres display a single absorption peak in the visible range between 510 nm and 550 nm. With increasing particle size, the absorption peak shifts to a longer wavelength and the width of the absorption spectra is related to the size distribution range.(79)

4.1.1.6.1.5. Gold nanorods

The synthesis of gold nanorods has been reported using a wide variety of strategies. Gold nanorods are typically synthesized using the template method, based on the electrochemical deposition of gold within the pores of nanoporous polycarbonate or alumina template membranes. [88] The diameter of the gold nanorods is determined by the pore diameter of the template membrane, while the length of the nanorods can be controlled through the amount of gold deposited within the pores of the membrane. A fundamental disadvantage of this method is the low yield since only one monolayer of nanorods is prepared. Formation of gold nanorods through electrochemical synthesis has also been reported. [89]

4.1.1.6.1.6. Gold nanoshells

Optical imaging, include those that uses gold nanoparticles as the contrast agents, has very limited applications in human studies, However, in the near-infrared region (NIR; 700–900 nm), the absorbance of all biomolecules reaches minimum which provides a relatively clear window for optical imaging. [154] By varying the composition and dimensions of the layers, gold nanoshells can be designed and fabricated with surface plasmon resonance(SPR) peaks ranging from the visible to the NIR region [155]For a given composition of gold nanoshell, the SPR peak can be tuned by changing the ratio of the core size to its shell thickness. [90]

4.1.1.6.1.7. Gold Nanocages

Gold nanocages with controllable pores on the surface have been synthesized via galvanic replacement reaction between truncated silver nanocubes and aqueous HAuCl4 [91]Silver nanostructures with controlled morphologies can be generated through polyol reduction, where AgNO3 is reduced by ethylene glycol to generate silver atoms and then nanocrystals or seeds. Subsequent addition of silver atoms to the seeds produces the desired nanostructures through controlling the silver seed crystalline structures in the presence of Polyvinylpyrolidone, a polymer that is capable of selectively binding to the (100) surface. The silver nanostructures, used as a sacrificial template, can then be transformed into gold nanostructures with hollow interiors via the galvanic replacement [92] The dimension and wall thickness of the resultant gold nanocages could be readily controlled, to very high precision, by adjusting the molar ratio of silver to HAuCl4. [78]

4.1.1.6.1.8. Applications of gold nanoparticles

Colloidal gold (Au) was discovered by scientists as early as in the fourth century B.C. Since then, colloidal Au solutions have been employed particularly for medical purposes. The first intravenous injection of Au solution was performed in 1880 to treat alcoholism and later for inoperable cancer patients. Au solution is also used to trigger specific biomolecular interactions in spinal-fluid and blood-serum proteins, on the other hand, isotope 198Au (half-life = 65 h) is employed in cancer care facilities for therapeutic use. [93]

Recent applications of colloidal Au are more versatile, including catalytic processes and electron transport in bio macromolecules, drug/imaging agent transport into cells by endocytosis pathway, investigation of cell motility, improvement of PCR efficiency and so

on. [94] Biomedical use of gold nanoparticles (AuNPs) was recently reviewed by Dykman et al. [95] where diagnosis, therapy, drug carrier and immunological properties of AuNPs are summarized as major applications. One of the advantageous physical properties of Au is its high X-ray absorption when employed in X-ray imaging.[94]

4.1.1.6.1.8.1 Therapeutic applications

Conventional strategies for cancer intervention include surgery, chemotherapy, and radiation therapy. [96]

New technologies have used the ability of tiny gold nanoparticles to collect specifically in a cancerous tumour by passing through the inherently leaky blood vessels attached to a tumour. Thus, when injected into a patient, there is a means by which a potent anticancer compound attached to a gold nanoparticle can be delivered directly and accurately to a tumour while avoiding surrounding healthy tissues. Such an effective drug delivery mechanism with reduced toxicity is considered to be a major step forward in cancer treatment; limiting side effects such as reduced immunity and hair loss taking advantage of their unique properties, most studies of gold nanoparticle-based cancer therapy have used photothermal therapy for the destruction of cancer cells or tumor tissue.[96]

4.1.1.6.1.8.2 Cell and phantom imaging

Most imaging studies using gold nanoparticles were carried out in cell culture, the versatile optical properties of gold nanoparticles have enabled optical imaging of cells and phantoms with a wide variety of contrast mechanisms. Functional cellular imaging around single molecules has been reported, taking advantage of the enhanced second harmonic signal by antibody conjugated gold nanospheres [97]

Cell and phantom imaging using gold nanoparticles serves as a proof-of-principle for their potential applications in live animals or cancer patients. It is unclear how these gold nanoparticles compare to other nanoparticles suitable for optical imaging, most notably quantum dots, [98]

Gold nanoparticles (GNPs) are emerging as one of the most promising contrast agents for computerized tomography (CT) due to their remarkable properties including high X-ray absorption coefficient, low cytotoxicity, tailored surface chemistry, excellent biocompatibility, and unique surface plasmon resonance. [99]

4.1.1.6.2. Titanium Dioxide Nanoparticles

TiO2 belongs to the family of transition metal oxides. There are four commonly known polymorphs of TiO2 found in nature: anatase (tetragonal) which produced as a white powder, brookite (orthorhombic), rutile(tetragonal), and TiO2 (B) (monoclinic) besides these polymorphs, two additional high-pressure forms have been synthesized from the rutile phase. These are TiO2 (II) with a PbO2 structure and TiO2 (H) [200] with a hollandite structure. [100-117]

4.1.1.6.3. Bi-metallic nanoparticles

Bimetallic or metal alloy nanoparticles can also exhibit superparamagnetic properties making them attractive candidates as MRI contrast agents or magnetic carriers for drug delivery. (101)

Typically obtained from a variety of processes, such as vacuum-deposition or solution phase synthesis, FePt nanoparticles are known to possess a chemically disordered face-centered cubic (fcc) or chemically ordered face-centered tetragonal (fct) structure, both of which result in near-equal atomic percentages of Fe and Pt (101-118)

4.1.1.7. Magnetic nanoparticles

4.1.1.7.1. Magnetic properties

Magnetic nanoparticles are spherical nanocrystals of 10–20 nm of size with a Fe2+ and Fe3+ core surrounded by dextran or PEG molecules. Their magnetic properties make them excellent agents to label biomolecules in bioassays, as well as MRI contrast agents. They are also amenable to surface functionalization for active targeting in vivo or for in vitro diagnostics (100)

Numerous forms of MNP with various chemical compositions have been proposed and evaluated for biomedical applications to exploit nanoscale magnetic phenomena, such as enhanced magnetic moments and superparamagnetism. Like other nanomaterial-based systems, advances in nanotechnology now allow for precise engineering of the critical features of these fine particles. Composition, size, morphology and surface chemistry can now be tailored by various processes to not only improve magnetic properties but also affect the behavior of nanoparticles in vivo (101-102)

In its simplest form, a biomedical MNP platform is comprised of an inorganic nanoparticle core and a biocompatible surface coating that provides stabilization under physiological conditions. Additionally, the application of suitable surface chemistry allows for the integration of functional ligands, this modular design enables MNPs to perform multiple functions simultaneously, such as in multi-modal imaging, drug delivery and real-time monitoring, as well as combined therapeutic approaches. (103)

The classification of a material's magnetic properties is based on its magnetic susceptibility (χ), which is defined by the ratio of the induced magnetization (M) to the applied magnetic field (H). In diamagnetic materials, the magnetic moment is antiparallel to H resulting in very small and negative susceptibilities (-10^{-6} to -10^{-3}). They do not retain magnetic properties when the external field is removed. Materials with magnetic moments aligned parallel to H and susceptibilities on the order of 10^{-6} to 10^{-1} are described as paramagnetic. (104)

While in ferri- and ferromagnetic materials, magnetic moments also align parallel to H, coupling interactions between the electrons of the material result in ordered magnetic states, i.e., magnetic domains, and large spontaneous magnetization. The susceptibilities of these materials depend on their atomic structures, temperature, and the external field H.(104)

At small sizes (on the order of tens of nanometers), ferri- or ferro-magnetic materials, such as MNPs, become a single magnetic domain and therefore maintain one large

magnetic moment. However, at sufficiently high temperatures (i.e., blocking temperature TB) thermal energy is sufficient to induce free rotation of the particle resulting in a loss of net magnetization in the absence of an external field. This superparamagnetic property, marked by the lack of remnant magnetization after removal of external fields, enables the particles to maintain their colloidal stability and avoid aggregation making it feasible for their use in biomedical applications. (100)

Although super paramagnetism is a favorable property of small particles, the reduction of particle size is not without some consequences. As particle sizes decrease, surface-to-volume ratios increase resulting in pronounced surface effects, such as non collinear spins, spin canting, and spin-glass-like behavior, which can significantly impact the magnetic properties of the material. (100)

4.1.1.7.2. Iron oxide nanoparticles

Colloidal iron oxide nanoparticles, such as SPIO and USPIO, have been the most extensively investigated MNPs for biomedical applications due to their excellent biocompatibility and ease of synthesis. Typically composed of nanocrystalline magnetite (Fe_3O_4) or maghemite (γFe_2O_3) protected with a polymeric coating, these ferrite nanoparticles possess a spinel crystal structure with oxygen ions forming a close-packed cubic lattice and iron ions located at interstices. In the case of Fe_3O_4, magnetization arises from electron hopping between the Fe^{2+} and Fe^{3+} ions that coexist at the octahedral sites.(105)

In addition to magnetic properties, the favorable biocompatibility and biodegradability of these MNPs have contributed greatly to their widespread use in biomedical applications. Upon metabolism, iron ions are added to the body's iron stores and eventually incorporated by erythrocytes as hemoglobin allowing for their safe use in vivo. (105)

Iron oxide nanoparticles have been produced by a variety of synthesis processes ranging from traditional wet chemistry solution-based methods to more exotic techniques such as laser pyrolysis or chemical vapor deposition, currently, SPIO and USPIO utilized or under investigation for clinical application as MRI contrast agents are predominately synthesized by an aqueous co-precipitation process in the presence of the coating material.(106-107)

In these hydrolytic processes, the control of the solution pH value and the presence of the coating material serving as a surfactant are critical to particle formation and properties. Unfortunately, magnetization can vary vastly among synthesis methods even within particles of similar size due to incorporation of impurities disrupting the crystal structure, as well as the surface effects described previously. Typically, M_s values of magnetite nanoparticles obtained by these methods are in the range of 30–50 emu/g, which is lower than the 90 emu/g reported for their bulk form. (107)

Recently, the use of high-temperature decomposition of organometallic precursors has been examined to produce iron oxide nanoparticles with marked improvements in size control, size distributions, and crystallinity. (186-187) in this process, the size of the nanoparticle is controlled by varying the reaction temperature or changing the metal precursor. Sizes could be further tuned by a seed-mediated growth process to obtain larger

particles. Utilizing this process, Sun et al. demonstrated the ability to synthesize highly uniform spherical Fe_3O_4 particles with size variation within 2 nm and mean diameters from 4 to 20 nm. (108)

One drawback of this approach is the use of hydrophobic oleic acid and oleylamine surfactants in the process which results in a hydrophobic coating on the particle surface necessitating additional modification to achieve nanoparticle solubility in aqueous media. Approaches such as the addition of an amphiphilic polymer or surface surfactant exchange have been utilized to overcome this problem. (109)

The need to improve magnetic properties for applications, such as molecular imaging, has generated interest in the development of metal doped iron oxides due to their enhanced magnetic properties. These spinel metal ferrites with a composition of MFe_2O_4, where M is +2 cation of Mn, Fe, Co or Ni, have been fabricated by various methods to tune specific magnetic properties (110)Recently, Lee et al. reported the synthesis and characterization of $MnFe_2O_4$, $FeFe_2O_4$, $CoFe_2O_4$, and $NiFe_2O_4$ by high-temperature reaction between divalent metal chloride and iron tris-2,4-pentadioate. (111)

Through comparison of various metal-doped ferrite nanoparticles, this group has demonstrated that $MnFe_2O_4$nanoparticles are nontoxic in vitro and possess higher magnetic susceptibility than magnetite nanoparticles, suggesting that they may be used as an ultrasensitive MR imaging probe. Cobalt and nickel ferrites have also been investigated recently for in vivo biomedical applications despite known toxicities of these elements. Baldi et al. (112) has examined the synthesis and coating of $CoFe_2O_4$ MNPs for use as magnetic nanocarriers. (113)

Utilizing a polyol-based synthesis method this group produced 5.4 nm particles coated with mono- and difunctional phosphonic and hydroxamic acids. Cobalt leakage was monitored through inductively coupled plasma atomic emission spectroscopy (ICP-AES) and found to correspond with quality of surface coverage by the attached ligand. Similarly, Rana et al. recently investigated the use of nanocrystalline $NiFe_2O_4$ as drug carriers (113)

4.1.1.7.3. Cobalt Nanoparticles

Cobalt-based nanoparticles reside among the most promising materials for technological applications like information storage devices, magnetic fluids, and catalysts Co is a well-known ferromagnetic material which is commonly used as an alloying element in permanent magnets. It exists in two forms: hexagonal close packed (HCP) and face centered cubic (FCC). HCP is the stable phase at room temperature, whereas FCC is stable at temperatures above450°C (193) Nanosized Co particles display a wide range of interesting size-dependent structural, electrical, magnetic, and catalytic properties (174)In particular, because of their large surface area, Co nanoparticles showed high chemical reactivity, which makes them suitable for catalysis. (114-115)

To have further applications of cobalt in different industries such as separation technology, information storage systems, catalysis, and biomedicine, nanoparticles are required to be discrete, identical in size and shape, and uniform in composition and crystal structure. (116)

4.1.1.7.4. Applications of magnetic nanoparticles

4.1.1.7.4.1. Diagnostic applications

4.1.1.7.4.1.1. Nuclear magnetic resonance imaging (NMR)

The development of the NMR imaging technique for clinical diagnosis has prompted the need for a new class of pharmaceuticals, so-called magnetopharmaceuticals.[117] These drugs must be administered to a patient in order to enhance the image contrast between normal and diseased tissue and/or and indicate the status of organ functions or blood flow.[118- 119]

A number of different agents have been suggested as potential NMR contrast agents. Most contrast agents used in NMR imaging studies to date have been paramagnetic. Superparamagnetic particles represent an alternative class of NMR contrast agents that are usually referred to as T2 (transversal relaxation time) or T2 contrast agents as opposed to T1 (longitudinal relaxation time) agents such as paramagnetic Gadolinium (III) chelates. The relaxation rate increase produced by magnetic particles is a contribution of several complex mechanisms. The particles possess very large magnetic moments in the presence of a static magnetic field, and dipolar interactions between the superparamagnetic cores and surrounding solvent protons result in an increase in both longitudinal and transverse relaxation rates, especially for particles with diameters below10 nm. [120]

4.1.1.7.4.2. Therapeutic applications

Hyperthermia, Hyperthermia is a therapeutic procedure used to raise the temperature of a region of the body affected by malignancy or other growths. It is administered together with other cancer treatments (multimodal oncological strategies). The rationale is based on a direct cell-killing effect at temperatures above 41–42˚C [121]

Modern clinical hyperthermia trials focus mainly on the optimization of thermal homogeneity at moderate temperatures (42–43˚C) in the target volume. The temperature increase required for hyperthermia can be achieved, among other methods, by using fine iron oxide magnetic particles. [122]

The physical principle for which a magnetic material can be heated by the action of an external alternating magnetic field are the loss processes that occur during the reorientation of the magnetization of magnetic materials with low electrical conductivity[123]

The advantage of magnetic hyperthermia is that allows the heating to be restricted to the tumour area. Moreover, the use of subdomain magnetic particles (nanometre-sized) is preferred instead multidomain (micron-sized) particles because nanoparticles absorb much more power at tolerable AC magnetic fields [124]

Hyperthermia and thermo ablation have been accomplished using capacitive or inductive coupling of RF fields (10–100 MHz), microwaves (> 300 MHz), ultrasound, lasers or external heat. [125]

4.1.1.7.4.2.1. Drug delivery

Since the pioneering concept proposed by Freeman et al [192] that fine iron particles could be transported through the vascular system and be concentrated at a particular point in the body with the aid of a magnetic field, the use of magnetic particles for the delivery of drugs or antibodies to the organs or tissues altered by diseases has become an attractive field of research. [126]

The process of drug localization using magnetic delivery systems is based on the competition between forces exerted on the particles by blood compartment, and magnetic forces generated from the magnet, i.e. applied field. When the magnetic forces exceed the linear blood flow rates in arteries (10 cm s−1) or capillaries (0.05 cm s−1), the magnetic particles are retained at the target site and maybe internalized by the endothelial cells of the target tissue. [126]

5. Computer Simulation Program (CST) Microwave Studio

CST MICROWAVE STUDIO is a fully featured software package for electromagnetic analysis and design in the high frequency range. it simplifies the process of creating the structure by providing a powerful graphical solid modeling front end which is based on the ACIS modeling kemel. After the model has been constructed, a fully automatic meshing procedure is applied before a simulation engine is started. [127]

CST promotes Complete Technology for 3D EM, gives a great flexibility in tackling a wide application range through the variety of available solver technologies. Beside the flagship module, the broadly applicable Time Domain solver and the Frequency Domain solver, CST MWS offers further solver modules for specific applications. [127]

A key feature of the CST microwave studio is a method on demand approach which gives the choice of simulator or mesh type that is best suited to a particular problem. [127]

The software contains several different simulation techniques (transient solver, frequency domain solver, integral equation solver, multilayer solver, asymptotic solver and eigenmode solver) to best suite various applications. The frequency domain solver also contains a specialized method for analyzing highly resonant structures such as filters. [127]